PHYSCON 2009, Catania, Italy, September, 1–September, 4 2009

A DIGITAL VERSION OF THE ADAPTIVE SPEED-GRADIENT-BASED CONTROL FOR COMPLEX VEHICLE DYNAMICS

Mario Alberto Jordan and Jorge Luis Bustamante
Argentinean Institute of Oceanography (IADO-CONICET) and
Department of Electrical Engineering and Computers,
Universidad Nacional del Sur (DIEC-UNS).
Florida 8000 CCT, E1. B8000FWB Bahía Blanca, Argentina.
e-mail: mjordan@criba.edu.ar

Abstract
In this paper a digital adaptive algorithm for path tracking of underwater vehicles in many degrees of freedom (up to six) was presented. It is based on speed-gradient laws and sampled-data models constructed with Adams-Bashforth approximations. Here it is assumed that no knowledge is required of the matrices of the Coriolis and centripetal forces, buoyancy, linear and quadratic damping. An analysis of stability for the path tracking problem is presented in which an optimal and, alternatively, a suboptimal control action are employed. The features of the approach are illustrated by means of a numerically simulated case study of a 6-degrees-of-freedom underwater vehicle maneuvering in the water column and sea bottom.

Key words
Underwater vehicle, nonlinear dynamics, sampled-data models, adaptive control, stability, residual set.

1 Introduction

In the past decade, new design tools and systematic design procedures has been developed to adaptive control for a set of general classes of nonlinear systems with uncertainties, for instance, integrator backstepping [Krstić, Kanellakopoulus and Kokotović, 1995], speed-gradient control [Fradkov, Miroshnik and Nikiforov, 1999], among others. In the absence of modeling uncertainties, adaptive controllers can achieve in general global boundedness, asymptotic tracking, passivity of the adaptation loop irrespectively of the relative degree, and systematic improvement of transient performance [Krstić, Kokotović and Kanellakopoulus, 1993].

Common applications in path tracking of unmanned vehicles are characterized by analog control approaches [Fossen, 1994; Inzartev, 2009]. The main reason is that the continuous-time nonlinear vehicle dynamics is typically available in the form of ordinary differential equations (ODEs). There is practically an absence of digital control approaches in this field. Moreover, the translation of ODE-based descriptions to time-discrete models when applying digital technology is too complex, unless a simple digitalization method, for instance the simple Euler's approximation, is carried out [Smallwood and Whitcomb, 2003; Cunha, Costa and Hsu, 1995]. This generally provides a good control performance if motions are rather slow. Another reason is the complexity of the dynamics itself, above all for path tracking problems in many degrees of freedom like in the case of underwater vehicles.

One particular characteristic of underwater vehicles is the high degree of uncertainty in the system matrices, namely of the inertia, Coriolis and centripetal forces, buoyancy and linear and nonlinear damping. Although the inertia matrix can be determined by means of simple experiments and calculations, this is not the case with the other ones that usually need expensive research and test facilities to be determined. So, the ability of the control system to catch information of the dynamics adaptively from measures would be highly desired in unmanned submarine vehicles [Jordán and Bustamante, 2009].

In this paper, we will describe the problem of digital controller design on the basis of highly precise sampled-data models. With this modelling tool the problem of high-performance guidance of underwater vehicles is introduced. The main feature of the digital control approach will be the ability of adaptation to uncertainties in the system matrices. Finally, a case study will illustrate the goodness of the our approach.

2 Vehicle Dynamics

Many systems are described as the conjugation of two ODEs in generalized variables, namely one for the kinematics and the other one for the inertia (see Fig. 1). The block structure embraces a wide range of vehicle systems like mobile robots (MR), unmanned aerial vehicles (UAV), spacecraft and satellite systems (SSS), autonomous underwater vehicles (AUV) or remotely operated vehicles (ROV), though with slight distinctive modifications in the structure among them.

In this paper underwater vehicles in six degrees of freedom (DOF), like ROVs, are focused. The degree of interconnection among states is complex and involved, with accentuated influence of state-dependent Coriolis and centripetal, drag and cable forces. So we can say that the results developed here for the most complex case also will comprehend the more simple cases of MR's, UAV's, SSS's and AUV's.

Let $\boldsymbol{\eta} = [x, y, z, \varphi, \theta, \psi]^T$ be the generalized position vector referred on a earth-fixed coordinate system termed O', with displacements x, y, z, and rotation angles φ, θ, ψ about these directions, respectively. Additionally let $\mathbf{v} = [u, v, w, p, q, r]^T$ be the generalized rate vector referred on a vehicle-fixed coordinate system termed O, oriented according to its main axes with translation rates u, v, w and angular rates p, q, r about these directions, respectively. The vector $\boldsymbol{\tau}$ is the generalized propulsion vector applied on O (also the future control action of a controller), $\boldsymbol{\tau}_c$ is a force perturbation applied on O (for instance the cable tug in ROVs), $\boldsymbol{\eta}_c$ is a perturbation of the position with respect to O', and finally $\mathbf{v}_c$ is a velocity perturbation with respect to O (for instance the fluid current in ROVs/AUVs or wind rate in UAVs).

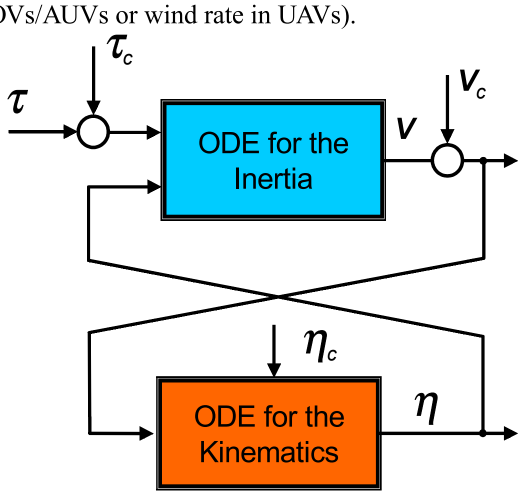

Figure 1. Physical model structure for vehicle dynamics.

The vehicle dynamics can be described by [Fossen, 1994] (see Fig. 1)

$$\dot{\mathbf{v}} = M^{-1}\Big(-C(\mathbf{v})\mathbf{v} - D(|\mathbf{v}|)\mathbf{v} + \mathbf{g}(\boldsymbol{\eta}) + \boldsymbol{\tau}_c + \boldsymbol{\tau}\Big) \quad (1)$$

$$\dot{\boldsymbol{\eta}} = J(\boldsymbol{\eta})(\mathbf{v} + \mathbf{v}_c), \quad (2)$$

where M, C and D are the inertia, the Coriolis-centripetal and the drag matrices, respectively, $\mathbf{g}$ is the buoyancy vector and J is the matrix expressing the transformation from the inertial frame to the vehicle-fixed frame. Finally, there may exist some perturbation $\boldsymbol{\tau}_c$ in the inertial system handled as an generalized force applied on O, for instance due to wind as in case of UAVs, fluid flow in AUVs, or cable tugs in ROVs.

For future developments in the controller design, it is necessary to factorize the system matrices into constant and variable arrays as [Jordán and Bustamante, 2008]

$$C(\mathbf{v}) = \sum_{i=1}^{6} C_i . \times C_{v_i}(\mathbf{v}) \quad (3)$$

$$D(|\mathbf{v}|) = D_l + \sum_{i=1}^{6} D_{q_i} \, |v_i| \quad (4)$$

$$\mathbf{g}(\boldsymbol{\eta}) = B_1 \, \mathbf{g}_1(\boldsymbol{\eta}) + B_2 \, \mathbf{g}_2(\boldsymbol{\eta}) \quad (5)$$

with ".×" being an element-by-element array product. The matrices C_i, D_l, D_{q_i}, B_1 and B_2 are constant and supposed unknown, while $C_{v_i}, \mathbf{g}_1$ and $\mathbf{g}_2$ are state-dependent and computable arrays and v_i is an element of $\mathbf{v}$.

As usually done, we will assume the rapid thruster dynamics is parasitic in comparison with the dominant vehicle dynamics [Jordán and Bustamante, 2008]. Besides, inertial, kinematics and positional perturbations of the cable, current and measures as in case of subaquatic vehicles are not considered in the analysis. Their influences in the dynamics are quite similar to them of the model uncertainties considered here.

3 Sampled-Data Model

Let us now regard an Adams-Bashforth approximation in the explicit form with a sampling period h [Butcher, 2003]. Thus, a one-step-ahead prediction of order s is

$$\mathbf{v}_{n+1} = \mathbf{v}_{t_n} + a_1 \mathbf{G}_{t_n} + ... + a_s \mathbf{G}_{t_{n-s+1}} \quad (6)$$

$$\boldsymbol{\eta}_{n+1} = \boldsymbol{\eta}_{t_n} + b_1 \mathbf{H}_{t_n} + ... + b_s \mathbf{H}_{t_{n-s+1}}, \quad (7)$$

where a_i and b_i are associated model coefficients of the linear combination obtained by using a Lagrange formula for polynomial interpolation, for instance, for $s = 4$ they are $a_1 = b_1 = \frac{55h}{24}$, $a_2 = b_2 = -\frac{59h}{24}$, $a_3 = b_3 = \frac{37h}{24}$, $a_4 = b_4 = -\frac{9h}{24}$. Moreover, $\mathbf{v}_{t_n}$ and $\boldsymbol{\eta}_{t_n}$, and similarly $\mathbf{G}_{t_i}$ and $\mathbf{H}_{t_i}$, are samples of the state vectors and the right-member functions of the ODE, respectively.

The sequence of samples $\mathbf{v}_{t_n}$ and $\boldsymbol{\eta}_{t_n}$ is referred here to as the exact sampled-data model of the system.

Now, taking samples of the right members of the ODE system (1)-(2) with (3)-(5) it yields

$$\mathbf{G}_{t_n} = M^{-1}\left(\sum_{i=1}^{6} C_i . \times C_{v_{i_{t_n}}} - D_l \mathbf{v}_{t_n} - \right. \quad (8)$$

$$\left. - \sum_{i=1}^{6} D_{q_i} \, |v_{i_{t_n}}| \mathbf{v}_{t_n} + B_1 \, \mathbf{g}_{1_{t_n}} + B_2 \, \mathbf{g}_{2_{t_n}} \right) + M^{-1} \boldsymbol{\tau}_n$$

$$\mathbf{H}_{t_n} = J_{t_n} \mathbf{v}_{t_n} \quad (9)$$

where $C_{v_{i_{t_n}}}$ means $C_{v_i}(\mathbf{v}_{t_n})$, $\mathbf{g}_{1_{t_n}}$ and $\mathbf{g}_{2_{t_n}}$ mean $\mathbf{g}_1(\boldsymbol{\eta}_{t_n})$ and $\mathbf{g}_2(\boldsymbol{\eta}_{t_n})$ respectively, $J_{t_n}^{-1}$ means $J^{-1}(\boldsymbol{\eta}_{t_n})$ and $v_{i_{t_n}}$ is an element of $\mathbf{v}_{t_n}$. Similar expressions can be obtained for the other sampled functions $\mathbf{G}_{t_i}$ and $\mathbf{H}_{t_i}$ in (6)-(7). Besides, the control action $\boldsymbol{\tau}$ is retained one sampling period h by a sample holder, so it is valid $\boldsymbol{\tau}_n = \boldsymbol{\tau}_{t_n}$.

As $\boldsymbol{\tau}_n$ is the control action to be determined, it is useful to construct the one-step-ahead prediction for $\mathbf{v}$ as

$$\mathbf{v}_{n+1} = \mathbf{v}_{t_n} + \left(a_1\overline{\mathbf{G}}_{t_n} + M^{-1}\boldsymbol{\tau}_n\right) + + \sum_{i=2}^{s} a_i\left(\overline{\mathbf{G}}_{t_{n-i+1}} + M^{-1}\boldsymbol{\tau}_{n-i+1}\right), \quad (10)$$

where clearly $\overline{\mathbf{G}}_{t_j} = \mathbf{G}_{t_j} - M^{-1}\boldsymbol{\tau}_j$.

The accuracy of one-step-ahead predictions is defined by the local model errors as

$$\varepsilon_{v_{n+1}} = \mathbf{v}_{t_{n+1}} - \mathbf{v}_{n+1} \quad (11)$$
$$\varepsilon_{\eta_{n+1}} = \boldsymbol{\eta}_{t_{n+1}} - \boldsymbol{\eta}_{n+1}, \quad (12)$$

with $\varepsilon_{\eta_{n+1}}, \varepsilon_{v_{n+1}} \in \mathcal{O}(h^s)$ and $\mathcal{O}$ being the order function that expresses the order of magnitude of the sampled-data model errors. Moreover, since $\mathbf{G}$ and $\mathbf{H}$ are Lipschitz continuous in the attraction domains in $\mathbf{v}$ and $\boldsymbol{\eta}$, then the samples, predictions and local errors all yield bounded. So, in absence of other errors other than $\varepsilon_{\eta_{n+1}}, \varepsilon_{v_{n+1}}$, it is valid the property $\mathbf{v}_{n+1} \to \mathbf{v}_{t_{n+1}}$ and $\boldsymbol{\eta}_{n+1} \to \boldsymbol{\eta}_{t_{n+1}}$ for $h \to 0$.

4 Design of a Digital Adaptive Controller

The next step is devoted to the design of a general digital adaptive controller based on speed-gradient control laws [Fradkov, Miroshnik and Nikiforov, 1999]. To this end let us suppose the control goal lies on the path tracking of both geometric and kinematic reference trajectories in discrete-time form specified in discrete time as $\boldsymbol{\eta}_{r_{t_n}}$ and $\mathbf{v}_{r_{t_n}}$, respectively.

Accordingly for the digital model translation, we try out the following definitions for the exact path errors [Conte and Serrani, 1999]

$$\breve{\boldsymbol{\eta}}_{t_n} = \boldsymbol{\eta}_{t_n} - \boldsymbol{\eta}_{r_{t_n}} \quad (13)$$
$$\breve{\mathbf{v}}_{t_n} = \mathbf{v}_{t_n} - J_{t_n}^{-1}\dot{\boldsymbol{\eta}}_{r_{t_n}} + J_{t_n}^{-1}K_p\breve{\boldsymbol{\eta}}_{t_n}. \quad (14)$$

where $K_p = K_p^T \geq 0$ is a design gain matrix affecting the geometric path error. Clearly, if $\breve{\boldsymbol{\eta}}_{t_n} \equiv \mathbf{0}$, then by (14) and (2), it yields $\mathbf{v}_{t_n} - \mathbf{v}_{r_{t_n}} \equiv \mathbf{0}$.

We now define a cost functional of the path error energy as

$$Q_{t_n} = \breve{\boldsymbol{\eta}}_{t_n}^T\breve{\boldsymbol{\eta}}_{t_n} + \breve{\mathbf{v}}_{t_n}^T\breve{\mathbf{v}}_{t_n}, \quad (15)$$

which is a positive definite and radially unbounded function in the error vector space.

We will then design a digital state feedback for the path tracking problem and afterward search for conditions to ensure the regulation of Q_{t_n} about zero as t_n tends to infinity for any small h.

Using (15), (11)-(12) and (13)-(14) the incremental value t_{n+1}, and after some calculations it yields

$$\Delta Q_{t_n} = Q_{t_{n+1}} - Q_{t_n} = \quad (16)$$
$$\Bigg[(I - b_1K_p)\breve{\boldsymbol{\eta}}_{t_n} + b_1\left(J_{t_n}\breve{\mathbf{v}}_{t_n} + \dot{\boldsymbol{\eta}}_{r_{t_n}}\right) + + \sum_{i=2}^{s} b_iJ_{t_{n-i+1}}\mathbf{v}_{t_{n-i+1}} + \boldsymbol{\eta}_{r_{t_n}} - \boldsymbol{\eta}_{r_{t_{n+1}}} + \boldsymbol{\varepsilon}_{\eta_{n+1}}\Bigg]^2 - \breve{\boldsymbol{\eta}}_{t_n}^2 +$$
$$+ \Bigg[\breve{\mathbf{v}}_{t_n} + J_{t_n}^{-1}\dot{\boldsymbol{\eta}}_{r_{t_n}} - J_{t_n}^{-1}K_p\breve{\boldsymbol{\eta}}_{t_n} - - J_{t_{n+1}}^{-1}\dot{\boldsymbol{\eta}}_{r_{t_{n+1}}} + J_{t_{n+1}}^{-1}K_p\breve{\boldsymbol{\eta}}_{t_{n+1}} + a_1\left(\overline{\mathbf{G}}_{t_n} + M^{-1}\boldsymbol{\tau}_n\right) + + \sum_{i=2}^{s} a_s(\overline{\mathbf{G}}_{t_{n-i+1}} + M^{-1}\boldsymbol{\tau}_{n-i+1}) + \boldsymbol{\varepsilon}_{v_{n+1}}\Bigg]^2 - \breve{\mathbf{v}}_{t_n}^2,$$

For the sake of simplicity in the notation the inner products for vectors such as $\mathbf{x}^T\mathbf{x}$ and $\mathbf{x}^TA\mathbf{x}$ were indicated as $\mathbf{x}^2$ and $A\mathbf{x}^2$, respectively.

As by similar designs of fixed controllers one can try to use $\boldsymbol{\tau}_n$ to compensate so many terms in (16) as possible. So one can conveniently split $\boldsymbol{\tau}_n$ into two terms as

$$\boldsymbol{\tau}_n = \boldsymbol{\tau}_{n_1} + \boldsymbol{\tau}_{n_2}, \quad (17)$$

where the first one is chosen with the aim of canceling almost all kinematics terms in (16) as

$$\boldsymbol{\tau}_{n_1} = M\Bigg(-K_v\breve{\mathbf{v}}_{t_n} - \frac{1}{a_1}J_{t_n}^{-1}\dot{\boldsymbol{\eta}}_{r_{t_n}} + + \frac{1}{a_1}J_{t_n}^{-1}K_p\breve{\boldsymbol{\eta}}_{t_n} + \frac{1}{a_1}J_{t_{n+1}}^{-1}\dot{\boldsymbol{\eta}}_{r_{t_{n+1}}} - \frac{1}{a_1}J_{t_{n+1}}^{-1}K_p\breve{\boldsymbol{\eta}}_{t_{n+1}} - - \widehat{\mathbf{G}}_{t_n} - \sum_{i=2}^{s}\frac{a_i}{a_1}\left(\widehat{\mathbf{G}}_{t_{n-i+1}} + M^{-1}\boldsymbol{\tau}_{n-i+1}\right)\Bigg), \quad (18)$$

with $K_v = K_v^T \geq 0$ another design matrix together with K_p, affecting the kinematic errors. Since systems matrices such as C_i, D_{q_i}, D_l, B_1 and B_2 are unknown, they are taken into account in (18) by means of estimations $\widehat{\mathbf{G}}_{t_j}$ for $\overline{\mathbf{G}}_{t_j}$ with j=n,...,$n-s$+1. Thus

$$\widehat{\mathbf{G}}_{t_j} = \sum_{i=1}^{6} U_{i\cdot} \times C_{v_{i_{t_j}}} - U_7\mathbf{v}_{t_j} - \sum_{i=1}^{6} U_{7+i}\,|v_{i_{t_j}}|\mathbf{v}_{t_j} + + M^{-1}U_{14}\,\mathbf{g}_{1_{t_j}} + M^{-1}U_{15}\,\mathbf{g}_{2_{t_j}}, \quad (19)$$

where the matrices U_i will account for every unknown system matrix in the partial control action $\boldsymbol{\tau}_{n_1}$ and their calculations will be made later by means of an adaptive law.

On the other hand, the second component $\boldsymbol{\tau}_{n_2}$ will result from solving (16) after having included (18) in ΔQ_{t_n}. So

$$\Delta Q_{t_n} = a(M^{-1}\boldsymbol{\tau}_{n_2})^2 + \mathbf{b}^TM^{-1}\boldsymbol{\tau}_{n_2} + c + + \breve{\boldsymbol{\eta}}_{t_n}^T a_1K_p(a_1K_p - 2I)\breve{\boldsymbol{\eta}}_{t_n} + + \breve{\mathbf{v}}_{t_n}^T a_1K_v(a_1K_v - 2I)\breve{\mathbf{v}}_{t_n} + + \mathbf{F}(\varepsilon_{\eta_{n+1}}, \varepsilon_{v_{n+1}}), \quad (20)$$

with

$$a = a_1^2 \quad (21)$$
$$\mathbf{b} = 2a_1\Bigg(\left((I - a_1K_v)\breve{\mathbf{v}}_{t_n}\right) + + \sum_{i=1}^{s} a_i(\mathbf{G}_{t_{n-i+1}} - \widehat{\mathbf{G}}_{t_{n-i+1}})\Bigg) \quad (22)$$

$$c{=}a_1^2\left(J_{t_n}\breve{\mathbf{v}}_{t_n}{+}\dot{\boldsymbol{\eta}}_{r_{t_n}}+\sum_{i=2}^{s}\frac{b_i}{a_1}J_{t_{n-i+1}}\mathbf{v}_{t_{n-i+1}}\right)^2 \quad (23)$$
$$+a_1\left(J_{t_n}\breve{\mathbf{v}}_{t_n}{+}\dot{\boldsymbol{\eta}}_{r_{t_n}}\right)^T\left(\boldsymbol{\eta}_{r_{t_n}}{-}\boldsymbol{\eta}_{r_{t_{n+1}}}\right)+$$
$$+\left(\boldsymbol{\eta}_{r_{t_n}}{-}\boldsymbol{\eta}_{r_{t_{n+1}}}\right)^T\left(\boldsymbol{\eta}_{r_{t_n}}{-}\boldsymbol{\eta}_{r_{t_{n+1}}}\right)+$$
$$+2\left(I-a_1K_p\right)\breve{\boldsymbol{\eta}}_{t_n}\left(a_1\left(J_{t_n}\breve{\mathbf{v}}_{t_n}{+}\dot{\boldsymbol{\eta}}_{r_{t_n}}\right)+\right.$$
$$\left.+\boldsymbol{\eta}_{r_{t_n}}{-}\boldsymbol{\eta}_{r_{t_{n+1}}}\right)+\sum_{i=1}^{s}a_i^2(\mathbf{G}_{t_{n-i+1}}{-}\widehat{\mathbf{G}}_{t_{n-i+1}})^2+$$
$$+2\sum_{i=1}^{s}a_i(\mathbf{G}_{t_{n-i+1}}{-}\widehat{\mathbf{G}}_{t_{n-i+1}})^T\left((I-a_iK_v)\breve{\mathbf{v}}_{t_n}\right)$$

and the vector function $\mathbf{F}$ fulfilling $\mathbf{F}(\varepsilon_{\eta_{n+1}},\varepsilon_{v_{n+1}})\rightarrow\mathbf{0}$ when $h\rightarrow 0$.

We could now search for the real roots of the polynomial $a\left(M^{-1}\boldsymbol{\tau}_{n_2}\right)^2+\mathbf{b}^TM^{-1}\boldsymbol{\tau}_{n_2}+c=0$ (if there exist), and then ensure $\Delta Q_{t_n}<0$ under certain conditions, at least inside an attraction domain excluding a residual set around zero (due to local model errors).

There exist here two inconveniences. The first one is we do not know the functions $\mathbf{G}_{t_j}$ in (22)-(23) to implement $\boldsymbol{\tau}_{n_2}$, even when $\boldsymbol{\tau}_{n_1}$ in (18) could be somehow implementable. The second one is we have not yet define any estimation $\widehat{\mathbf{G}}_{t_j}$ of these functions that can ensure $\Delta Q_{t_n}<0$.

This last point is addressed in the next section, while the first one is satisfied by simply choosing new coefficients termed $\bar{a},\bar{\mathbf{b}}$ and $\bar{c}$ of $a,\mathbf{b}$ and c, respectively, with expressions

$$\bar{a}=a \quad (24)$$
$$\bar{\mathbf{b}}=2a_1(I{-}a_1K_v)\breve{\mathbf{v}}_{t_n} \quad (25)$$
$$\bar{c}=c-\sum_{i=1}^{s}a_i^2(\mathbf{G}_{t_{n-i+1}}{-}\widehat{\mathbf{G}}_{t_{n-i+1}})^2+ \quad (26)$$
$$-2\sum_{i=1}^{s}a_i(\mathbf{G}_{t_{n-i+1}}{-}\widehat{\mathbf{G}}_{t_{n-i+1}})^T\left((I-a_iK_v)\breve{\mathbf{v}}_{t_n}\right).$$

Now, they all are computable and serve to select real roots of $\bar{a}\left(M^{-1}\boldsymbol{\tau}_{n_2}\right)^2{+}\bar{\mathbf{b}}^TM^{-1}\boldsymbol{\tau}_{n_2}{+}\bar{c}=0$ for implementing $\boldsymbol{\tau}_{n_2}$. So it is valid

$$\boldsymbol{\tau}_{n_2}=\frac{-M}{2\bar{a}}\bar{\mathbf{b}}\pm\frac{M}{2\bar{a}}\sqrt{\frac{\bar{\mathbf{b}}^T\bar{\mathbf{b}}-4\bar{a}\bar{c}}{6}}\mathbf{o}, \quad (27)$$

with $\mathbf{o}$ a vector with all the six elements equal to one. In order to achieve minimal energy of the control action or eventually to avoid saturation, one can choose the solution with minimal norm.

So the control action to be applied to the vehicle system is $\boldsymbol{\tau}_n=\boldsymbol{\tau}_{n_1}+\boldsymbol{\tau}_{n_2}$ with the two components given in (18) and (27), respectively.

If, on the contrary, there are no real roots, one can choose the real part of (27). The implicances of this choice in the stability of the control system will be analyzed later.

5 Adaptive Laws

We will employ adaptive laws of the kind speed-gradient for determining the controller matrices U_i in $\widehat{\mathbf{G}}_{t_j}$. Our approach is an extension for digital controllers of the continuous-time forms proposed in [Fradkov, Miroshnik and Nikiforov, 1999]. To this end we define at t_n

$$U_{i_n}\triangleq U_{i_{n-1}}-\Gamma_i\frac{\partial\Delta Q_{t_n}}{\partial U_{i_n}}, \quad (28)$$

with a gain matrix $\Gamma_i=\Gamma_i^T\geq 0$ and $\frac{\partial\Delta Q_{t_n}}{\partial U_{i_n}}$ being a gradient matrix satisfying

$$\frac{\partial\Delta Q_{t_n}}{\partial U_i}=\frac{\partial}{\partial U_i}\left(\frac{\left(\bar{\mathbf{b}}{-}\mathbf{b}\right)^T\left(\bar{\mathbf{b}}{-}\mathbf{b}\right)}{2\bar{a}}\mp\right. \quad (29)$$
$$\left.\mp\frac{\bar{\mathbf{b}}^T{-}\mathbf{b}^T}{2\bar{a}}\sqrt{\bar{\mathbf{b}}^T\bar{\mathbf{b}}{-}4\bar{a}\bar{c}{+}c{-}\bar{c}}\right).$$

Here the expression for ΔQ_{t_n} was developed for the solution for $\boldsymbol{\tau}_{n_2}$ in (27).

Now $\bar{\mathbf{b}}$, c and $\bar{c}$ depend on the different controller matrices U_i's through the functions $\widehat{\mathbf{G}}_{t_j}$'s in (19). We can see from (29) that ΔQ_{t_n} will be always convex in the matrices U_i. This means that for an arbitrary element u_i of any controller matrix U_i in ΔQ_{t_n} with any pair of values u_1 and u_2 of u_i, the inequality

$$\Delta Q_{t_n}(u_1)-\Delta Q_{t_n}(u_2)\leq\frac{\partial\Delta Q_{t_n}}{\partial u_1}\left(u_1-u_2\right), \quad (30)$$

is fulfilled.

6 Stability Analysis

In this section we attempt to show convergence of error trajectories to a residual set in the path tracking problem.

Let us first define particular values for the controller matrices U_i's and referred them to as U_i^*'s. So, using the unknown system matrices (3)-(5) and (8) following matrices are proposed

$$U_i^*=C_i,\ \text{with}\ i=1,...6 \quad (31)$$
$$U_7^*=D_l \quad (32)$$
$$U_i^*=D_{q_i},\ \text{with}\ i=8,...13 \quad (33)$$
$$U_{14}^*=B_1 \quad (34)$$
$$U_{15}^*=B_2\ . \quad (35)$$

Then we consider ΔQ_{t_n} for a particular control action constructed with constant matrices $U_i=U_i^*$. In this situation it can be deduced from (25)-(26) and with $\mathbf{G}_{t_j}{=}\widehat{\mathbf{G}}_{t_j}$ that $\left(\bar{\mathbf{b}}{-}\mathbf{b}\right)=\mathbf{0}$ and $c{-}\bar{c}=0$. So this particular functional yields

$$\Delta Q_{t_n}^*=\breve{\boldsymbol{\eta}}_{t_n}^Ta_1K_p\left(a_1K_p-2I\right)\breve{\boldsymbol{\eta}}_{t_n}+ \quad (36)$$
$$+\breve{\mathbf{v}}_{t_n}^Ta_1K_v\left(a_1K_v-2I\right)\breve{\mathbf{v}}_{t_n}+$$
$$+\mathbf{F}(\varepsilon_{\eta_{n+1}},\varepsilon_{v_{n+1}}).$$

It is noticing that $\Delta Q_{t_n}^*<0$, at least in an attraction domain equal to

$$\mathcal{B}=\left\{\breve{\boldsymbol{\eta}}_{t_n},\breve{\mathbf{v}}_{t_n}\in\mathcal{R}^6\cap\mathcal{B}_0\right\}, \quad (37)$$

with $\mathcal{B}_0$ a residual set around zero when the design matrices satisfy the conditions

$$\frac{2}{a_1}I>K_p\geq 0 \quad (38)$$
$$\frac{2}{a_1}I>K_v\geq 0. \quad (39)$$

The residual set $\mathcal{B}_0$ depends on $\varepsilon_{\eta_{n+1}}$ and $\varepsilon_{v_{n+1}}$, and clearly it is the null point at the limit when $h \to 0$.

Let us consider at this point a Lyapunov function

$$V_{t_n} = \Delta Q_{t_n} + \frac{1}{2} \sum_{i=1}^{15} \sum_{j=1}^{6} \left(\tilde{\mathbf{u}}_n^T\right)_{i_j} \Gamma_i^{-1} \left(\tilde{\mathbf{u}}_n\right)_{i_j} - \quad (40)$$

$$-\frac{1}{2} \sum_{i=1}^{15} \sum_{j=1}^{6} \left(\tilde{\mathbf{u}}_{n-1}^T\right)_{i_j} \Gamma_i^{-1} \left(\tilde{\mathbf{u}}_{n-1}\right)_{i_j}$$

with $\left(\tilde{\mathbf{u}}_n\right)_{i_j} = \left(\mathbf{u}_n - \mathbf{u}_n^*\right)_{i_j}$, where $\mathbf{u}_n$ and $\mathbf{u}_n^*$ are vectors corresponding to the column j of the matrices U_{i_n} and $U_{i_n}^*$, respectively. Moreover after some calculations we attain

$$V_{t_n} = \Delta Q_{t_n} + \frac{1}{2} \sum_{i=1}^{15} \sum_{j=1}^{6} \left(\Delta \mathbf{u}_n^T\right)_{i_j} \Gamma_i^{-1} \left(\tilde{\mathbf{u}}_n + \tilde{\mathbf{u}}_{n-1}\right)_{i_j} \quad (41)$$

$$= \Delta Q_{t_n} + \sum_{i=1}^{15} \sum_{j=1}^{6} \left(\Delta \mathbf{u}_n^T\right)_{i_j} \Gamma_i^{-1} \left(\tilde{\mathbf{u}}_n\right)_{i_j} -$$

$$-\frac{1}{2} \sum_{i=1}^{15} \sum_{j=1}^{6} \left(\Delta \mathbf{u}_n^T\right)_{i_j} \Gamma_i^{-1} \left(\Delta \mathbf{u}_n\right)_{i_j}$$

$$\leq \Delta Q_{t_n} - \sum_{i=1}^{15} \sum_{j=1}^{6} \left(\frac{\partial \Delta Q_{t_n}}{\partial U_{i_n}}\right)_j^T \left(\tilde{\mathbf{u}}_n\right)_{i_j}$$

$$\leq \Delta Q_{t_n}^* < 0 \text{ in } \mathcal{B} \cap \mathcal{B}_0,$$

with $\Delta \mathbf{u}_n$ a column vector of $U_{i_n} - U_{i_{n-1}}$. At the first inequality, the adaptive law (28) for the column vector $\left(\Delta \mathbf{u}_n\right)_{i_j}$ was replaced by the column vector $-\Gamma_i \left(\frac{\partial \Delta Q_{t_n}}{\partial U_{i_n}}\right)_j$ in the right member. At the second inequality, the convexity property of ΔQ_{t_n} in (30) was applied for any pair $(U_1 = U_{i_n}, U_2 = U_i^*)$.

This analysis has proved convergence of the error paths when real roots exist for the equation: $a \left(M^{-1} \boldsymbol{\tau}_{n_2}\right)^T M^{-1} \boldsymbol{\tau}_{n_2} + \mathbf{b}^T M^{-1} \boldsymbol{\tau}_{n_2} + c = 0$.

If on the contrary $4ac > \mathbf{b}^T \mathbf{b}$ occurs at some time t_n, one chooses the real part of (27), which is the one that minimizes the value of the function $a \left(M^{-1} \boldsymbol{\tau}_{n_2}\right)^T M^{-1} \boldsymbol{\tau}_{n_2} + \mathbf{b}^T M^{-1} \boldsymbol{\tau}_{n_2} + c$. So a suboptimal control action is employed instead equal to

$$\boldsymbol{\tau}_{n_2} = \frac{-M}{2a} \mathbf{b}, \quad (42)$$

and yields the functional $\Delta Q_{t_n}^* + c - \frac{1}{4a} \mathbf{b}^T \mathbf{b}$. It can be shown from the expressions in (22) and (23) that there exist a suffiently small sampling time h that makes the $\Delta Q_{t_n}^* \leq \frac{1}{4a} \mathbf{b}^T \mathbf{b} - c$, it is the control stable for a suboptimal control action $\boldsymbol{\tau}_{n_2}$ applied constantly. So, the suboptimal $\boldsymbol{\tau}_{n_2}$ provide in fact a large attraction domain with a appropriate selection of K_p and K_v, however with a larger residual set than $\mathcal{B}_0$ depending also on the magnitude of $\left(c - \frac{1}{4a} \mathbf{b}^T \mathbf{b}\right)$, apart from $\varepsilon_{\eta_{n+1}}$ and $\varepsilon_{v_{n+1}}$.

7 Case Study: Maneuver on the Seabottom

In order to illustrate the features of the adaptive approach, let us consider the path tracking problem for the underwater vehicle described in Fig. 2. The vehicle has to navigate along a geometric path with a prescribed kinematics in time. This consists of different motions in the water column which are typically employed in sampling maneuvering over the sea floor.

The digital control algorithm is implemented according to (27), (42) and adaptive laws which are given in (28). The sample time h was chosen 0.1 sec. and the simplest Adams-Bashforth model of $s = 1$ was employed.

The previous knowledge of the system dynamics only contemplates the inertia matrix. The other system matrices are completely unknown. The self-tuning phase and the stationary phase are described in Figs. 3 and 4 (on the left and right, respectively) for the position vector $\boldsymbol{\eta}$ with elements $x, y, z, \varphi, \theta, \psi$, and for the kinematics vector $\mathbf{v}$ with elements u, v, w, p, q, r, respectively.

One notices on the left hand that the transient phase elapses a short period of about 5 sec. During the whole navigation, the optimal and suboptimal solutions for $\boldsymbol{\tau}_n$ have taken turns in time. However, this alternation appears much more frequently in the stationary state than in the adaptation phase, i.e., when the path errors are quite small. These conforms the residual set that results with an order of magnitude of about 10^{-4}.

The all-round performance reached with the proposed adaptive approach is judged as a high one in the numeric simulations and comparable with the analogous control system obtained at the limit for $h \to 0$ [Jordán and Bustamante, 2007].

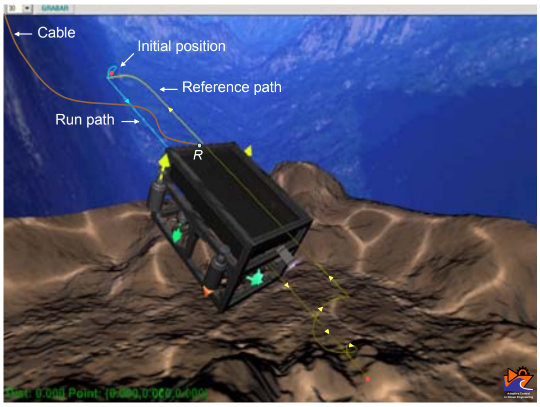

Figure 2. Path tracking of an underwater vehicle in the column and sea bottom.

8 Conclusions

In this paper a digital adaptive algorithm for path tracking of vehicles in many degrees of freedom (up to six) was presented. It is based on speed-gradient laws and sampled-data models constructed with Adams-Bashforth approximations.

The control system design results more complex than in the case of continuous-time controllers. Even when the translation of the analogous phenomenological ODE system of the vehicle dynamics to Adams-Bashforth approximations of any order looks uncomplicated, the derivation of a digital speed-gradient adaptive control action is not straightforward. The main reason is that the design functional of the path tracking errors has a quadratic form, in contrast with the linear form in the continuous-time case for the same dynamics. However, the adaptive digital control system performs comparatively so good as the analogous one with the advantage that its implementation in computer is much more adequate.

Though the adaptive controller design does not require of the knowledge of the matrices of the Coriolis and centripetal, buoyancy, linear and quadratic damping, it is however demanded a-priori the knowledge of the mass matrix. This is perhaps not a serious restriction, because this could be estimated with simple experiments, which does not occur with the remaining system matrices.

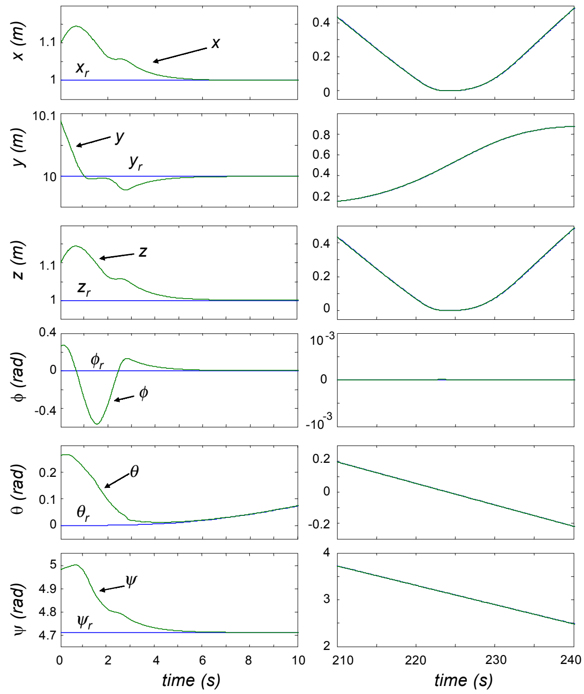

Figure 3. Evolution of the geometric paths.

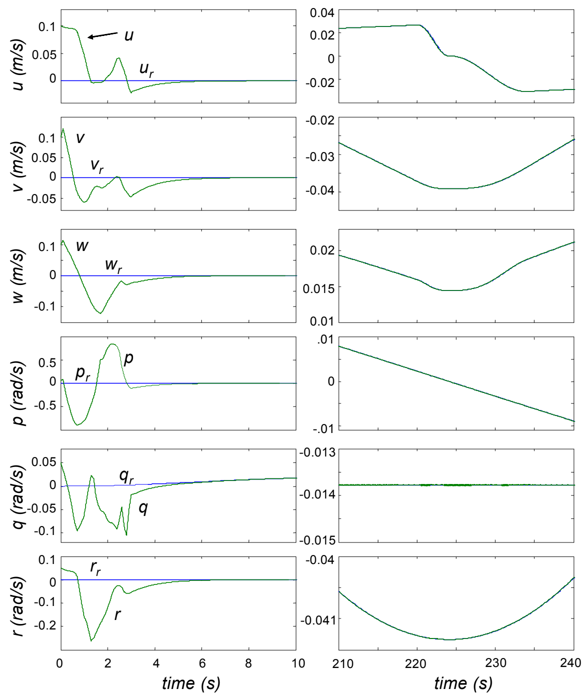

Figure 4. Evolution of the kinematics paths.

Besides, an analysis of stability of the adaptive control system for path tracking was presented in which an optimal and, alternatively, a suboptimal control action were employed. The results indicate that the adaptive controller is able to conduct both geometric and kinematic error paths inside a residual set that depends on the model error magnitude of the Adams-Bashforth approximation.

Finally, an illustration of the features of the approach was described by means of a numerically simulated case study of a 6-degrees-of-freedom underwater vehicle maneuvering in the water column and sea bottom. Future works consider the analysis of the algorithm robustness when noise perturbations are included in the system.

References

Butcher, J. C. (2003). *Numerical Methods for Ordinary Differential Equations.* John Wiley and Sons. Chistester, England.

Conte, G. and Serrani, A. (1999) Robust nonlinear motion control for AUVs. *IEEE Robotics & Automation Magazine*, **6**(2), pp. 62,33-38

Cunha, J. P. V. S, Costa, R. R. and Hsu, L. (1995) Design of a High Performance Variable Structure Position Control of ROV's. *IEEE J. of Oceanic Engineering*, **20**(1), pp. 42-55.

Fossen, T. I. (1994). *Guidance and Control of Ocean Vehicles*. John Wiley&Sons. New York.

Fradkov, A. L., Miroshnik, I. V. and Nikiforov, V. O. (1999). *Nonlinear and adaptive control of complex systems*, Kluwer Acad. Pub.

Inzartev, A. V. (Ed.) (2009).*Underwater Vehicles.* In-Tech.Vienna, Austria.

Jordán, M. A. and Bustamante, J. L. (2007). An Adaptive Control System for ROVs in Discrete Sampling Missions with Time-Optimal Characteristics. In *2007 American Control Conference*, New York , USA, July 11-13, 2007, pp. 894-899.

Jordán, M. A. and Bustamante, J. L. (2008) Guidance of Underwater Vehicles with Cable Tug Perturbations Under Fixed and Adaptive Control Modus. *IEEE J. of Oceanic Engineering*, **3**(4), 2008, pp. 579 - 598.

Jordán, M. A. and Bustamante, J. L. (2009) Adaptive Control for Guidance of Underwater Vehicles. In *Underwater Vehicles,* A.V. Inzartev (Ed.). In-Tech. Vienna, Austria. Chapter 14, pp. 251-278.

Krstić, M. , Kanellakopoulus, I. and Kokotović, P. V. (1995) *Nonlinear and adaptive control design*. John Wiley and Sons, Inc. New York.

Krstić, M., Kokotović, P. V. and Kanellakopoulus, I. (1993) Transient performance improvement with a newclass of adaptive controllers. *Syst. Control Lett.,* **21**, pp. 451-461.

Smallwood, D. A. and Whitcomb, L. L. (2003) Adaptive Identification of Dynamically Positioned Underwater Robotic Vehicles. *IEEE Trans. on Control Syst. Technology*, **11**(4), pp. 505-515.